

1+ / N+ METHOD: NUMERICAL SIMULATION STUDIES AND EXPERIMENTAL MEASUREMENTS ON THE SPIRAL1 CHARGE BREEDER

A. Annaluru[†], P. Delahaye, M. Dubois, P. Jardin, O. Kamalou, L. Maunoury, A. Savalle,
V. Toivanen and P. Ujic, GANIL, F-14076 Caen, France
E. Traykov, IPHC, F-67200 Strasbourg, France

Abstract

In the framework of the SPIRAL1 facility, the R & D of charge breeding technique is of primary interest for optimizing the yields of radioactive ion beams (RIBs). This technique involves the transformation of mono-charged ion beams into multi-charged ion beams by operating an Electron Cyclotron Resonance (ECR) charge breeder (CB). During the SPIRAL1 commissioning, experimental studies have been performed in order to understand the transport of the beam through the CB with and without ECR plasma. Numerical simulations including ion optics and some ECR plasma features have been developed to evaluate ion losses during the ion transport through the CB with and without a simplified model of the ECR plasma.

INTRODUCTION

The SPIRAL1 facility at GANIL is dedicated to produce and accelerate the stable and radioactive ion beams which are delivered to physicists for nuclear experimental studies. Extending their research on exotic nuclei properties far from stability, an upgrade has been undertaken at SPIRAL1 to extend the range of post-accelerated exotic beams as well as to provide low energy (keV) radioactive beams to the future DESIR (Désintégration, Excitation et Stockage d'Ions Radioactifs) experimental area. Different Target Ion Source System (TISS) based on a forced electron beam induced arc discharge (FEBIAD) type mono-charged ion source [1] has been chosen to provide 1+ beams of condensable elements with high efficiency. The 1+ beams from TISS are mass analyzed and transported to the 14.5 GHz SPIRAL1 ECR charge breeder (CB), which increases the charge state charge of the radioactive ions from 1+ to N+. The extracted high charge state ions are mass analyzed and post accelerated to CIME cyclotron (Cyclotron d'Ions de Moyenne Energie) [2]. Figure. 1 shows the 3D cross-section of the charge breeder placed in the Low Energy Beam Transport (LEBT) between the TISS and the CIME. In the injection side of the CB the beam is focused with an electrostatic quadrupole triplet and the extracted beam is focused with an einzel lens. The charge breeder has gone through several modifications which are reported in [3, 4], and experimental charge breeding results are presented in [5]. During its operation, a few technical changes have been done in the configuration of the charge breeder: the position of two soft iron rings has been modified to optimize the axial magnetic field and the optimiza-

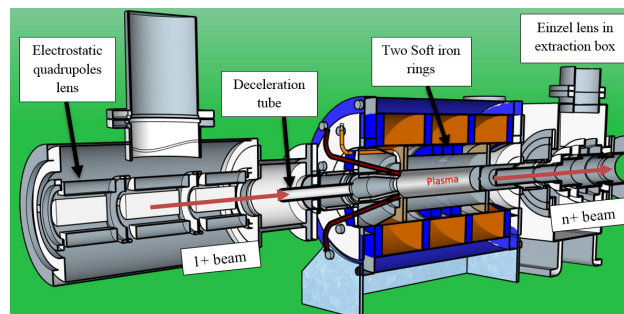


Figure 1: 3D view of ECR charge breeder connected with injection and extraction systems.

tion of the deceleration tube position to study its effect on beam stability and charge breeding efficiency. Experimental studies on LEBT transport and charge breeding efficiencies for $^{23}\text{Na}^+$ and $^{23}\text{Na}^{2+}$ have been carried out to understand the ion losses and 1+ capture processes by ECR plasma. A rough analysis on the experimental studies is described in the following sections by introducing a simplified ECR plasma model utilizing SIMION 3D. The results obtained from the simulations are presented and compared with the experimental ones.

EXPERIMENTAL ACTIVITIES WITH SPIRAL1 ECR CHARGE BREEDER

Modification of Axial Magnetic Field

In ECR ion source based charge breeders, the “Minimum-B” magnetic field structure is created by 2 or 3 independent solenoids (axial field) and hexapole (radial field) magnets enclosed in an iron yoke. In this configuration, the magnetic field is minimum at the center of plasma chamber and increases in all directions. The Minimum-B configuration is essential to form a closed resonance surface in the plasma chamber where ECR condition is fulfilled.

In SPIRAL1 charge breeder, the axial magnetic field (B) can be adjusted with the center coil and two movable soft iron rings (R1 and R2) placed around the hexapole as shown in Fig. 2. Magnetic field calculations were performed with RADIA [6] to study the axial magnetic field profile by adjusting the rings to different positions. Before the modification, the two rings were placed at extraction end of CB. When the rings are pushed to different positions, significant variations were observed in the size of ECR zone in axial direction. Axial magnetic field profiles for different rings position are

[†] arun.annaluru@ganil.fr

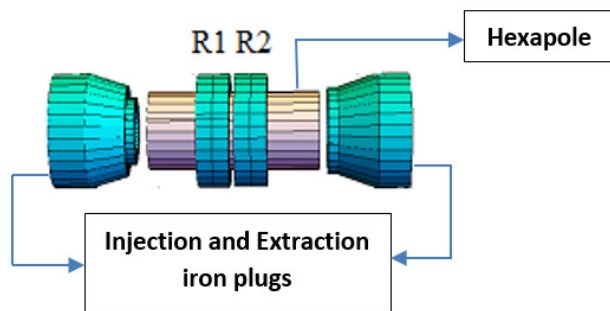


Figure 2: Position of two soft iron rings (R1 and R2) around the hexapole.

shown in Fig. 3. From these B field plots, the soft iron rings

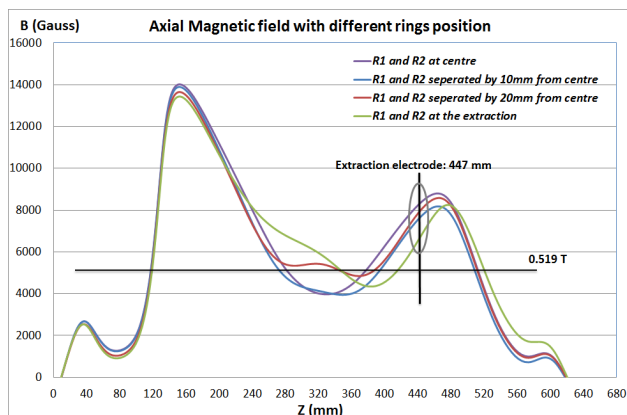


Figure 3: Axial B fields with different positions of the two soft iron rings. a) two rings touched at center (purple) b) rings separated by 10 mm from the center (Blue) c) rings separated by 20 mm from the center (Red) d) two rings at the extraction of CB. Center refers to the center of plasma chamber (320 mm).

Table 1: $^{39}\text{K}^{9+}$ Efficiency Measured at Different Rings Positions. Center Is referred As Center of Plasma Chamber (320 mm)

Rings position	$^{39}\text{K}^{9+}$ efficiency
R1 and R2 at extraction	7.44 %
R1 and R2 touched at center	10.08 %
R1 and R2 separated by 20mm from center	10.88%
R1 and R2 separated by 10mm from center	11.6%

separated by 10 mm from the center of the plasma chamber has been chosen as the best configuration. Because, the size of the ECR zone is larger, compared to the other configurations. Implementing this configuration can increase the ion and electron confinement times in the plasma volume consequently enhance the production of highly charged ions.

To test the theoretical hypothesis, this modification has been executed during the charge breeding of $^{39}\text{K}^{9+}$. During these measurements, Helium was used as buffer gas in CB. Table 1 shows the charge breeding efficiency of $^{39}\text{K}^{9+}$ with different positions of the two iron rings. As a result, with the best configuration charge breeding efficiency of $^{39}\text{K}^{9+}$ has been increased by a factor of 1.5 when compared with initial position of the rings.

Transmission Efficiencies of $^{39}\text{K}^+$ and $^{23}\text{Na}^+$

The thermionic ion gun was used to produce the 1+ ion beams of $^{39}\text{K}^+$ (420 nA) and $^{23}\text{Na}^+$ (550 nA) at 10 kV and 15 kV respectively, with emittance (4σ) of 50π .mm.mrad (non-normalized) through the 14.5 GHz SPIRAL1 ECR charge breeder at SPIRAL1. The 1+ and n+ beam lines have been tuned to achieve maximum ion beam current, up to the Faraday cup (FC_{1+}) and likewise to the Faraday cup (FC_{n+}), which is placed after the charge breeder. The starting point for the optics tuning was defined from TraceWin simulation in order to achieve high transmission efficiencies in LEBT. By turning OFF the charge breeder (without plasma and high voltage), the transmission efficiency of 80% and 78% on $^{39}\text{K}^+$ and $^{23}\text{Na}^+$ were recorded at faraday cup (FC_{n+}). The axial B field configuration was: at injection $B_{inj} = 1.41$ T, at center $B_{min} = 0.42$ T, at extraction $B_{ext} = 0.5$ T.

Charge breeding of ^{23}Na

Table 2: Parameters Used in Charge Breeding of Sodium

Parameters	Charge breeding of Na
Magnetic field at injection (B_{inj})	1.41 T
Magnetic field at minimum (B_{min})	0.42 T
Magnetic field at extraction (B_{ext})	0.91 T
RF power (Watt)	540 W

Hereafter, the experiments were performed with helium as buffer gas in ECR charge breeder, which is observed to be the best for optimizing the charge breeding efficiencies of high charge states of K and Na [7]. Please refer to Table 2 for typical values used for charge breeding of Na. The thermionic ion gun was used to produce the $^{23}\text{Na}^+$ beam which was injected into SPIRAL1 charge breeder with an intensity of 550 nA at 20 kV. The emittance (4σ) value for injected $^{23}\text{Na}^+$ is 30π .mm.mrad (non-normalized). By proper tuning of ΔV , the charge breeding efficiencies of 0.82%, 3.23%, 3.57% and 1.2% were recorded on Na^{2+} , Na^{7+} , Na^{8+} and Na^{9+} , respectively. ΔV was tuned between 6 V and 8 V. During the measurements, the tuning was observed to be very sensitive with the potential difference (ΔV) between 1+ source and charge breeder. The ΔV value for maximum achieved efficiency is same for high charge states of sodium, which was similar when compared with results obtained for sodium with LPSC PHOENIX charge breeder [8].

Effect of Deceleration Tube Position on Charge Breeding Efficiency

In SPIRAL1 charge breeder, the charge breeding efficiencies for $^{23}\text{Na}^+$ and $^{23}\text{Na}^{8+}$ were recorded at different positions of the deceleration tube. Observing the geometry sub-plot in Fig. 4, the optimum position is found at a distance of 21 mm from the injection plug of CB. The Na^+ beam measured downstream from the charge breeder was stable at the optimum position and became unstable when the tube was moved to the ends. It is also clear that, Na^{8+} plot shows the similar tendency with the position of the deceleration tube when compared with Na^+ . To summarize, this parameter is critical for the beam stability and has shown a clear effect on charge breeding efficiency.

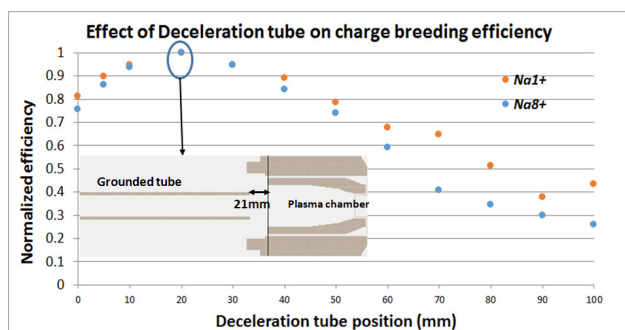


Figure 4: Effect of deceleration tube position on Na^+ and Na^{8+} charge breeding efficiency. At 0 mm, the position of the tube is inside the charge breeder. Measured Na^+ and Na^{8+} curves are normalized to 1 from 8.14% and 3.65%.

Effect of Injected Beam Emittance On Charge Breeding Efficiency

The 20 kV $^{23}\text{Na}^+$ beam was injected into SPIRAL1 charge breeder with an emittance of $30 \pi \cdot \text{mm} \cdot \text{mrad}$ (non-normalized). The ΔV was optimized in order to reach a Charge breeding efficiency of 3.53% on $^{23}\text{Na}^{8+}$. The in-

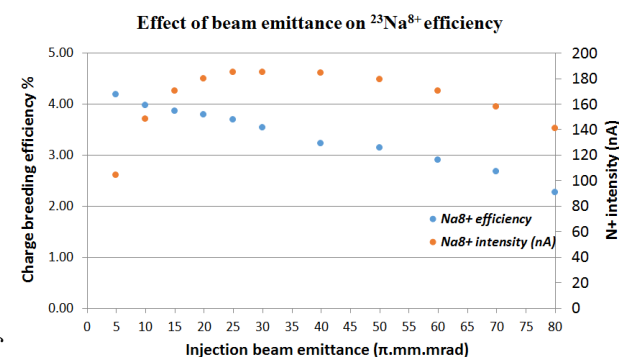


Figure 5: effect of beam emittance on Na^+ and Na^{8+} charge breeding efficiency.

jected beam emittance was then varied from $5 \pi \cdot \text{mm} \cdot \text{mrad}$ to $80 \pi \cdot \text{mm} \cdot \text{mrad}$ by adjusting a set of slits between the 1+ source and the CB. Figure. 5 depicts influence of injection

beam emittance on $^{23}\text{Na}^{8+}$ efficiency and n+ intensity. Observing the intensity plot, a significant drop in beam currents is recorded at low emittance. This drop correlates with the collimating parts of the beam that are actually injected into plasma. Beam currents steadily increases with increase in emittance, which correlates parts of the beam that cannot be injected into the plasma are collimated away by the slits. At higher emittance ($> 60 \pi \cdot \text{mm} \cdot \text{mrad}$), a small drop in beam currents has been observed. It suggests that perhaps increased ion losses in the injection region effecting the injection efficiency. The observed charge breeding efficiency trends steadily decrease with increase in emittance and n+ beam currents.

NUMERICAL SIMULATION STUDIES ON ECR CHARGE BREEDER

Simulation Description

Numerical simulations were performed using SIMION 3D [9] to evaluate the ion losses during the transport of 1+ beam through the charge breeder with and without a simplified model of the ECR plasma. These cases correspond with the situations where the CB is switched off (shooting through mode) and on (charge breeding mode).

The main ingredients of this simulation are; precise geometry of SPIRAL1 charge breeder, ion optics (deceleration tube, electrostatic quadrupole lens, CB extraction einzel lens) and 3D magnetic field of the charge breeder (calculated from RADIA). The electric fields are calculated in SIMION by applying potentials to the geometry electrodes. The geometry is arranged according to the LEPT line in SPIRAL1 as shown in Fig. 6. Additional features are added to the simulations according to our requirements (e. g., plasma potential). For initiating the ions in the simulation, a Matlab code has been developed, which can generate the initial ions using twiss parameters. The energy and mass of 1+ ions can be changed in the code according to our requirements. Furthermore, ion losses in the simulated system are monitored with a dedicated Lua user program.

Ion Transport Through Charge Breeder Without Plasma

In this case, $^{39}\text{K}^+$ and $^{23}\text{Na}^+$ ions at energy of 10 keV and 15 keV are injected into the charge breeder with emittance of $50 \pi \cdot \text{mm} \cdot \text{mrad}$. The emittance used for this case is similar to the experimental once. Figure. 6 shows the simulation of $^{39}\text{K}^+$ ions transported through the CB. In both cases (K^+ and Na^+), It was observed that up to 20% of the initial ions were lost at the extraction aperture.

Ion Transport Through Charge Breeder Plasma

To investigate this process, a simplified plasma model has been introduced in the simulation, which allows to reproduce the trends of experimental ΔV curves. A few regions of fixed potentials are included inside the plasma chamber to approximate the potential distribution in the plasma volume, including the potential dip in the core plasma (see

Content from this work may be used under the terms of the CC BY 3.0 licence (© 2018). Any distribution of this work must maintain attribution to the author(s), title of the work, publisher, and DOI.

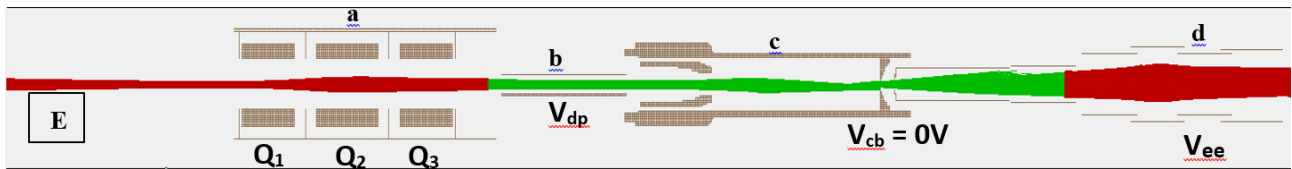


Figure 6: The geometry of electrostatic quadrupole lens (a), deceleration tube (b), ECR charge breeder (c) and extraction einzel lens (d) used in the ion transport simulation. At the point E, 10000 $^{39}\text{K}^+$ ions are initiated with the energy of 10 keV and simulated through ECR charge breeder. The total ions extracted from charge breeder are counted after the extraction system.

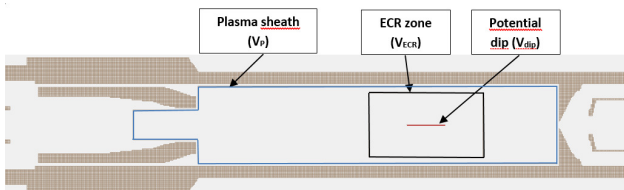


Figure 7: The geometry of ECR charge breeder with the ECR plasma features and ion optics used in the study of 1+ capture processes.

Fig. 7). The plasma potential (V_p) and potential applied at ECR zone (V_{ECR}) are always equal in all cases in order to confine the potential dip inside the resonance zone. The simplified plasma model presented in this paper does not include collisions or other interactions between the ions.

Before initiating the ions in the simulation, the plasma potential (V_p) and potential applied at ECR zone (V_{ECR}) are adjusted to higher value than the potential of charge breeder (V_{cb}) so that the incoming ions are decelerated due to positive plasma potential. The potential dip is always considered as $V_{dip} = V_{ECR} - 1 \text{ V}$. The plasma potential of 10 V has been chosen in order to reproduce the ΔV curves. However, based on experimental optimum ΔV results we know that the plasma potential in reality is lower, most likely below 8 V. But in order to simulate the trends, this discrepancy should not be critical.

Ions are initiated with an emittance of $30 \pi \cdot \text{mm} \cdot \text{mrad}$ at an energy of 20 keV. The ΔV curves in the simulation is defined as the potential difference between the charge breeder and injection energy of 1+ ions. In order to initiate Na^{2+} ion beam in this simulation, a Lua programme has been written to change the charge state of Na^+ to Na^{2+} after entering into ECR zone without disturbing the kinetic energy of ions.

SIMULATION RESULTS AND DISCUSSION

With the transmission simulations (CB off), Transmission efficiencies of 84% and 79% for K^+ and Na^+ were recorded after the extraction system, which are very similar to the experimental results reported in the previous sections. From the observations, 100% transmission has been achieved up to the entrance of CB. The ion losses were observed only at the extraction aperture. Ion losses significantly increase with increase in V_{cb} .

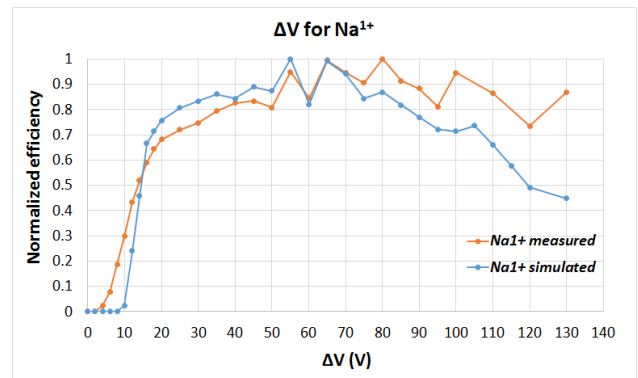


Figure 8: Normalized efficiencies of Na^+ as a function of ΔV . Measured and simulated curves are normalized to 1 from 28% and 24%.

The second part of the numerical simulation concerned the extraction of Na^+ and Na^{2+} through CB plasma volume. From the observations, the recorded simulated curve seems to shift towards higher ΔV when compared with experimental curves. In order to find the best agreement with the experimental curves, the emittance of 1+ beam has been varied to $20 \pi \cdot \text{mm} \cdot \text{mrad}$ by keeping the same twiss parameters. Observing Fig. 8 and Fig. 9, similar trends were recorded for Na^+ and Na^{2+} . At low ΔV , most of the ions are reflected back to the deceleration tube due to positive plasma potential (e.g. 85% of ions with ΔV between 9 - 10 V). When ΔV is at 55 V, the maximum of the Na^+ is obtained, and the ion losses at the entrance of plasma chamber significantly decreased to 15%. Moreover, real discrepancies can be seen after 50V and higher, which was also observed in Na^+ experimental curves. In case of Na^{2+} , the ions are initiated at the core of ECR zone. The observed trends between the simulated and measured data agree, but the simulation seems to significantly over-estimate the efficiency compared to the measured values. This is probably due to the very simplified 1+ \rightarrow 2+ conversion model implemented in the simulations.

The discrepancies observed in the simulations shows that the 1+ (and maybe 2+) beam traversing through the plasma chamber exhibits a periodic focusing/defocusing behavior due to the solenoid field [10], and consequently the phase of this motion at the extraction aperture influences the transmission. Furthermore, as this motion is ion energy dependent, varying ΔV or V_{cb} influences the phase at the extraction aper-

Content from this work may be used under the terms of the CC BY 3.0 licence (© 2018). Any distribution of this work must maintain attribution to the author(s), title of the work, publisher, and DOI.

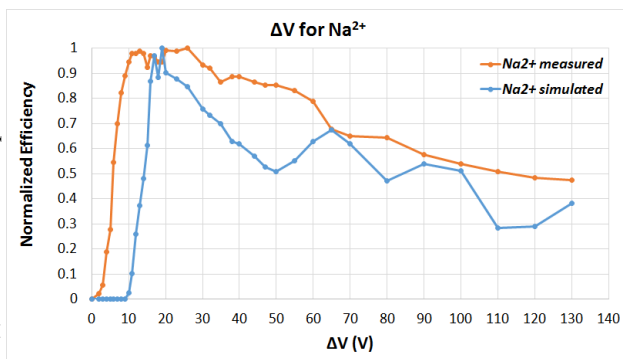


Figure 9: Normalized breeding efficiency of Na^{2+} as a function of ΔV . Measured and simulated curves after are normalized to 1 from 0.9% and 21%.

ture and therefore the transmission. Thus this phenomenon can explain some of the features seen in the simulation results (oscillating transmission). As similar oscillations are present in measured data, it suggests that perhaps similar effects takes place in reality.

SUMMARY AND PERSPECTIVES

Simulations revealed that the ion losses at the extraction aperture are mostly due to the beam oscillations in the charge breeder. The transmission efficiencies obtained from the simulations show good agreement with the experimental results. The ΔV plots for Na^+ and Na^{2+} obtained from a rough analysis performed with the simplified ECR plasma model has shown similar trends when compared with the experimental curves. In future, the simulation model presented in this paper will be improved by distributing the Na^{2+} ions randomly in the core of ECR plasma instead of using a conversion from $1+$ to $2+$ at a fixed axial position. Simultaneously, the ΔV plots for Na^+ and Na^{2+} will be calculated with a numerical simulation code called MCBC (Monte Carlo Charge Breeding Code) which can model the capture and charge breeding of a beam of ions injected into a plasma [11]. The ΔV plots

obtained from SIMION 3D and MCBC will be compared for further investigation regarding the $1+$ capture process by ECR plasma. To complete this analysis, additional experimental data will be gathered from Mg (using He buffer gas) and K (using He and O_2 buffer gas) charge breeding efficiency (also charge breeding time) measurements. This approach can show a possible way to determine the tendency of charge breeding parameters which influences the $1+$ ion capture efficiency by the ECR plasma.

REFERENCES

- [1] O. Kamalou *et al.*, in *Proc. of the 13th International Conference on Heavy Ion Accelerator Technology*, pp.20-22 (2015)
- [2] M. Duval *et al.*, in *Proc. of the 14th International Workshop on Magnet Technology, MT-14 Tampere, Finland, June 11-16 (1995)*.
- [3] P. Delahaye *et al.*, *Nuclear Instruments and Methods in Physics Research, A* vol. 693, p. 104 (2012).
- [4] L. Maunoury *et al.*, *Review of Scientific Instruments*, vol. 85, p. 02A504 (2016).
- [5] L. Maunoury *et al.*, in *Proc. of the 22nd International Work-shop on ECR Ion Sources*, Busan, South Korea, 28th August-1st September (2016).
- [6] RADIA magnetic field simulation code, <http://www.esrf.eu/Accelerators/Groups/InsertionDevices/Software/Radia>
- [7] L. Maunoury *et al.*, *Review of Scientific Instruments*, vol. 87, pp. 02B508 (2016).
- [8] T. Lamy *et al.*, in *Proc. of the 18th International Workshop on ECR Ion Sources*, Chicago, Illinois, US, September 15-18, 2008.
- [9] SIMION Ion and Electron Optics Simulator, <http://www.simion.com>
 ScientificInstrumentServices, Inc. (SIS)
- [10] V. Kumar, *American Journal of Physics*, vol. 77, pp. 737 (2009).
- [11] JS. Kim *et al.*, *Review of Scientific Instruments*, vol. 78, pp. 103503, (2007).